

Edge effect enhanced photo-thermionic emission from a carbon nanotubes array

Chi Li, Zhenjun Li, Ke Chen, Bing Bai, and Qing Dai^{a)}

Nanophotonics Research Division, CAS Center for Excellence in Nanoscience, National Center for Nanoscience and Technology, Beijing 100190, China

(Received 22 December 2016; accepted 10 February 2017; published online 1 March 2017)

Employing optical field enhancement at the edges of the nanostructures, an enhanced photo-thermionic emission (PTE) was obtained from a well-defined carbon nanotube (CNT) cluster array. Compared with the un-patterned carbon nanotube film, the PTE from the CNT cluster array was enhanced 10 times at the same laser intensity. The concept was proved by the computer simulation as well. We believe that an edge effect enhanced CNT PTE emitter is of great potential for application in next-generation portable and inexpensive vacuum electronic devices. *Published by AIP Publishing.* [<http://dx.doi.org/10.1063/1.4977189>]

Electron sources are the key component of vacuum devices, such as displays,¹ electron microscopy,² ion thrusters,³ free electron lasers,⁴ and microwave amplifiers.⁵ Among various excitation methods, photo-induced electron emission (PEE) sources have attracted great attention due to their properties including fine modulation, high spatial and temporal resolution, and remote control capability, which make them appealing for next generation vacuum electronic devices. Much effort has been paid to investigate the PEE performances of nano-materials due to their unprecedented ability to concentrate the incoming light into deep-sub-wavelength volumes.^{6–8} At the edges and protrusions of nanostructures, the optical field can be significantly enhanced, leading to an enhanced PEE. Among various nanomaterials, carbon nanotubes (CNTs) are of great interest^{9,10} due to their several features: high aspect ratio, small tip radius, high mechanical and thermal stabilities, and high electrical conductivity.^{11–14} Specially, high efficient photo-induced thermionic emission (PTE)^{15–18} has been realized from the high density CNT film.

In this work, employing an optical field enhancement effect at the edges of the emitters, we attempt to obtain enhanced PTE from a well-defined CNT cluster array. The concept of our experiment is schematically illustrated in Fig. 1(a), and it relies on the controlled fabrication of a vertically aligned patterned CNT cluster array on a silicon substrate, illuminated by a continuous wave (CW) laser with a central wavelength of 650 nm. At the edges of the CNT cluster apices, the optical field and the laser intensity are greatly enhanced due to the geometry.^{8,19,20} Consequently, the photo-thermal effect is more efficient at the edges, leading to an enhanced PTE compared to an un-patterned CNT film.

Vertically aligned patterned CNT cluster arrays were grown on a highly doped *n*-type silicon chip by the chemical vapor deposition (CVD) method. First, the silicon substrate was coated with an Al (10 nm)/Fe (1 nm) multilayer catalyst by sputtering and patterned by photolithography. Then, the substrate was heated to 700 °C at a pressure of 10^{−2} mbar. During heating, ammonia gas was introduced to etch the

catalyst film into small particles.^{21,22} Acetylene was chosen as the carbon source and introduced into the deposition chamber once the temperature had reached 750 °C. The growth process lasted for 5 min, resulting in nearly 80 μm thickness of CNTs. The side view of the fabricated CNT array was characterized by Scanning Electron Microscopy (SEM, Hitachi, S-4800) and is shown in Figs. 1(b) and 1(c). The CNTs in the array were uniform, dense, well-aligned, and perpendicular to the substrate. Vertical self-alignment of CNTs has been proven to be the result of Van der Waals interactions between neighboring CNTs.¹² The pitch between two adjacent CNT clusters is 20 μm. For comparison, un-patterned CNT film samples were synthesized using the same growth condition.¹⁶

The experiment setup is schematically illustrated in Fig. S1 (supplementary material). PTE from CNT samples was triggered by a CW laser with a central wavelength of 650 nm using a simple laser diode. A laser power meter (Spectra-Physics 407 A) was used to measure and calibrate the laser power. The light was normally incident on the CNT arrays via side illumination with a 30° incidence angle. The light was focused to a 0.5 mm² spot on the CNT samples. The samples were mounted in a high-vacuum chamber (10^{−8} Torr). An Indium-Tin Oxide (ITO) glass anode was placed 3 mm

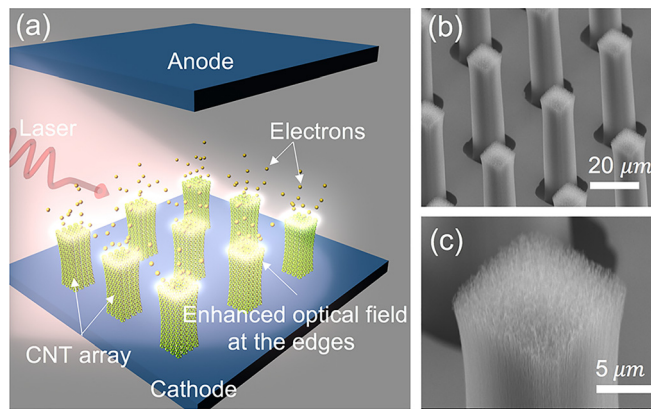


FIG. 1. (a) Concept of the edge effect enhanced PTE from the patterned CNT array. SEM images of the CNT cluster array (b) and apex of a single CNT cluster (c).

^{a)} Author to whom correspondence should be addressed. Electronic mail: daiq@nanoctr.cn

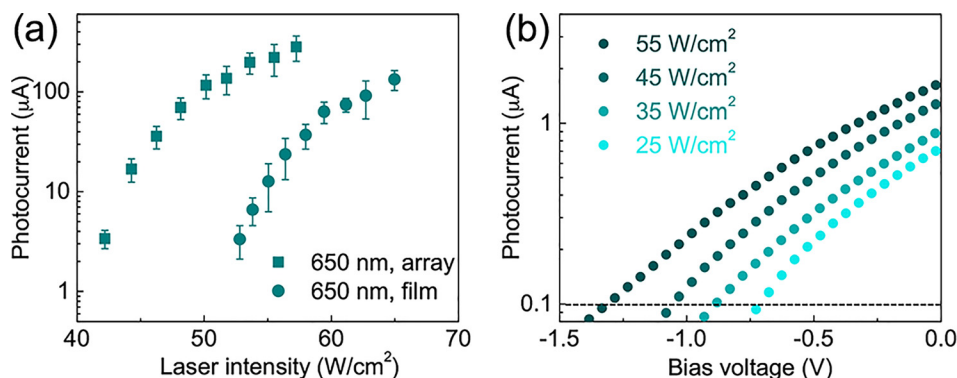


FIG. 2. (a) Emission current density as a function of laser intensity at a bias voltage of 100 V for both the CNT cluster array and the un-patterned CNT film. (b) The dependency of the photocurrent on negative bias voltage, suggesting an increased cutoff electron energy with the laser intensity.

away from the cathode to prevent possible thermal damage to the ITO film induced by the photothermal effect on the CNTs. A Keithley 2612 source measurement unit was used to bias the anode and measure the continuous photoemission current. An oscilloscope was used to measure the pulsed emission current and the pulsed laser simultaneously. A signal generator was employed to drive the CW laser and achieve laser pulses.

The measured electron photoemission currents as a function of the laser intensities at a bias voltage of 100 V are displayed in Fig. 2(a). According to the room temperature electrostatic field emission testing, no visible field emission current was detected at a voltage below 100 V, which excludes the contribution of field emission current to the total emission current. Three other mechanisms can explain electron emission from laser irradiation at sub-turn-on field, namely, single photon photoemission (SPPE), strong field photoemission (SFPE), and PTE itself. SPPE can be excluded since the energy of a single photon of either wavelength (650 nm corresponds to ~ 2.0 eV) is not high enough to allow the electrons to overcome the CNT vacuum barrier (4.39 eV).¹⁶ SFPE (including multi-photon photoemission and optical field emission) is also not expected to occur because it normally requires a laser intensity higher than GW/cm^2 with an optical field higher than 0.1 GV/m, which must be produced by an ultra-fast laser.^{8,23} In our case, the laser intensity is lower than $200 \text{ W}/\text{cm}^2$, while the optical field intensity is less than $0.1 \text{ V}/\mu\text{m}$, which is far from enough for SPPE even with the edge optical field enhancement (which is lower than 100, as will be discussed below).^{8,23,26} The low optical electric field is expected to have a negligible effect on the vacuum barrier as well as on the emission current. In our previous study, we demonstrated that the PTE mechanism from a carbon nanotube film was constituted by photo-thermionic emission by measuring the light emission spectrum of the excited area.¹⁶ In this work, to further confirm the mechanism, we measured the cutoff voltage (V_c , defined as the bias voltage at an emission current of $0.1 \mu\text{A}$) as a function of laser intensities by employing the retarding field method,²⁴ as shown in Fig. 2(b). The experimental data suggested that the maximum electron kinetic energy (corresponding to $e|V_c|$) increased with increasing local temperature (in proportion to laser intensity), which is in good agreement with theoretical predictions of thermionic emission²⁵ and support the PTE prediction.

At a laser intensity of $\sim 58 \text{ W}/\text{cm}^2$, an emission current of $\sim 300 \mu\text{A}$ was measured for the CNT cluster array, while at the same intensity, the measured emission current was only

$\sim 30 \mu\text{A}$ for the un-patterned CNT film. One may argue that the greatly enhanced electron emission may in principle be attributed to variations in the illuminated surface area when moving from the film to the array. However, geometrical calculations (Fig. S2, supplementary material) revealed that the illuminated area of the array is a little smaller than that of the film, which means that the increase of emission current arises only from the optical enhancement due to the edge effect.

To clarify that the observed enhanced PTE from the patterned CNT cluster array is originated from such an edge enhancing effect, we calculated the optical field distribution on the CNT cluster apex. The calculations were performed by the finite element method, employing Maxwell's equations in the radio frequency module of a commercially available software COMSOL Multi-physics. The simulation process has been widely reported.^{8,26} The optical parameters were extracted from Ref. 27. Fig. 3 shows the calculated optical field distribution (electric field component) of a single CNT cluster at an incident laser intensity of $55 \text{ W}/\text{cm}^2$, corresponding to an electric field component of $\sim 5.5 \text{ V}/\text{mm}$. The optical field enhancement factor at the edge reaches ~ 8 , corresponding to a laser intensity magnification of ~ 64 , which is much higher than that of other areas. These results indicate that the optical field is predominantly concentrated at the periphery of each cluster of the CNTs, which act as major emission sites. Therefore, the highly efficient PTE from the CNT array can be attributed to the edge enhancement effect.

The time response of an electron emitter is an important parameter for measuring its maximum rate of on/off switching. A fast time response is highly desirable for the applications of electron emitters, which require a fast alternating

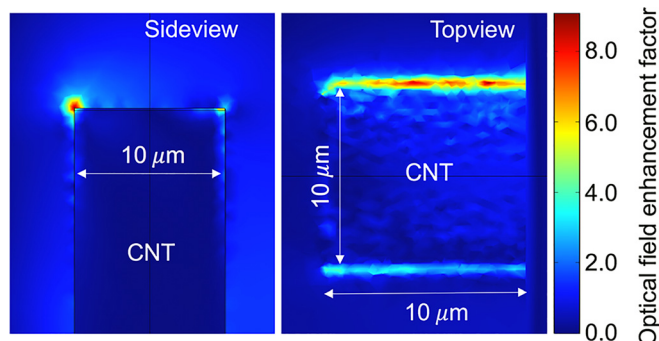


FIG. 3. Simulation of optical field enhancement on a single CNT cluster apex.

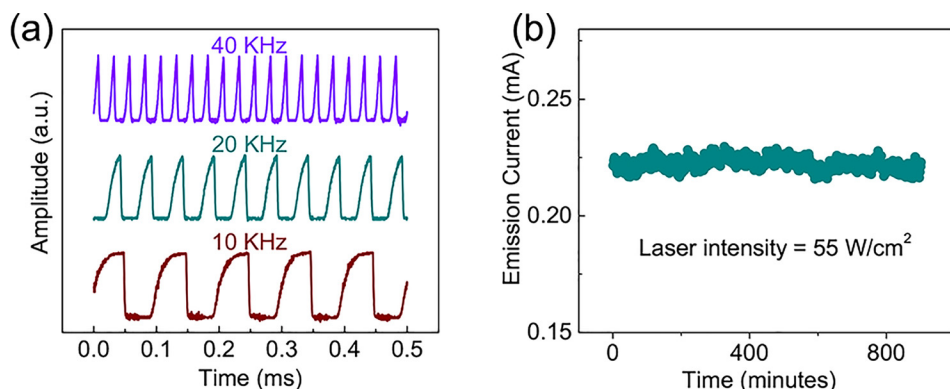


FIG. 4. (a) Laser On/off testing, showing high uniformity of emission pulses. (b) Dependency of emission current on time, showing a low fluctuation and long lifetime.

electron beam. For example, in a high level computed tomography (CT), the required on/off frequency of the X-ray source is higher than 4 kHz. As can be seen from Fig. 4(a), a fast response frequency up to 40 kHz can be achieved for the PTE from a CNT array, indicating a turn-on time shorter than $10\ \mu\text{s}$ and a turn-off time on the nanosecond time scale. The fast time response of electron emission from the CNT array is attributed to the enhanced local intensities at the edge of the CNT cluster, which means that the temperature increases much faster at the edge than in other areas of the array in the same time-domain. The timescale of the photo-thermal process can be theoretically estimated to fall in the order of several hundred femto-seconds. It should be noted that, in our case, the main limitation is constituted by the slow response of the laser. Further research on the intrinsic timescale of PTE from a CNT array can be carried out with an ultrafast laser (nanosecond or picosecond). In addition, operation of PTE from the CNT cluster array continuously for more than 12 h (Fig. 4(b)) without obvious degradation and fluctuation highlights the potential of the present CNT emitter to operate as long lifetime and stable electron sources.

In summary, PTE from a CNT array is significantly enhanced due to the optical near-field enhancement at the edge of the CNT cluster apexes. Compared with traditional bulk thermionic emitters, CNT-PTE presents a number of advantages including micro scale size, high working frequency, and the possibility to obtain remote control via an inexpensive laser diode. At the same time, the process shows a high emission stability. Based on this concept, tip-enhanced PTE from single or few CNT emitters can be a topic of interest for further studies in order to develop nanoscale thermionic emitters. As the theoretical response time has been proven to fall within the femtosecond scale, CNT-PTE is also a good candidate for next generation ultrafast electron sources.

See [supplementary material](#) for (1) the detailed schematic diagram of the experiment setup and (2) a simple geometrical calculation of the illuminated area on the patterned CNT cluster array and un-patterned film.

This work was supported by the National Basic Research Program of China (Grant no. 2016YFA0202000, 2015CB932400, 2016YFA0300903), the National Natural Science Foundation of China (Grant no. 11427808, 51372045), and the International Science and Technology Cooperation Project (No. 2014DFR10780, China.)

- ¹W. B. Choi, D. S. Chung, J. H. Kang, H. Y. Kim, Y. W. Jin, I. T. Han, Y. H. Lee, J. E. Jung, N. S. Lee, G. S. Park, and J. M. Kim, *Appl. Phys. Lett.* **75**(20), 3129–3131 (1999).
- ²A. Tomomura and T. Komoda, *J. Electron Microscopy (Tokyo)* **22**(2), 141–147 (1973).
- ³S. Marcuccio, A. Genovese, and M. Andrenucci, *J. Propul. Power* **14**(5), 774–781 (1998).
- ⁴G. L. Carr, M. C. Martin, W. R. McKinney, K. Jordan, G. R. Neil, and G. P. Williams, *Nature* **420**(6912), 153–156 (2002).
- ⁵K. B. K. Teo, E. Minoux, L. Hudanski, F. Peauger, J. P. Schnell, L. Gangloff, P. Legagneux, D. Dieumegard, G. A. J. Amaratunga, and W. I. Milne, *Nature* **437**(7061), 968–968 (2005).
- ⁶G. Herink, D. R. Solli, M. Gulde, and C. Ropers, *Nature* **483**(7388), 190–193 (2012).
- ⁷M. Kruger, M. Schenk, and P. Hommelhoff, *Nature* **475**(7354), 78–81 (2011).
- ⁸M. E. Swanwick, P. D. Keathley, A. Fallahi, P. R. Krogen, G. Laurent, J. Moses, F. X. Kartner, and L. F. Velasquez-Garcia, *Nano Lett.* **14**(9), 5035–5043 (2014).
- ⁹D. A. Lyashenko, E. D. Obraztsova, A. N. Obraztsov, and Y. P. Svirko, *Phys. Stat. Sol. B* **243**(13), 3505–3509 (2006).
- ¹⁰A. N. Obraztsov and V. I. Kleshch, *J. Nanoelectron. Optoelectron.* **4**(2), 207–219 (2009).
- ¹¹R. Patra, S. Ghosh, E. Sheremet, M. Jha, R. D. Rodriguez, D. Lehmann, A. K. Ganguli, O. D. Gordan, H. Schmidt, S. Schulze, D. R. T. Zahn, and O. G. Schmidt, *J. Appl. Phys.* **116**, 164309 (2014).
- ¹²S. S. Fan, M. G. Chapline, N. R. Franklin, T. W. Tomblor, A. M. Cassell, and H. J. Dai, *Science* **283**(5401), 512–514 (1999).
- ¹³P. Liu, Y. Wei, K. L. Jiang, Q. Sun, X. B. Zhang, S. S. Fan, S. F. Zhang, C. G. Ning, and J. K. Deng, *Phys. Rev. B* **73**(23), 235412 (2006).
- ¹⁴T. L. Westover, A. D. Franklin, B. A. Cola, T. S. Fisher, and R. G. Reifenberger, *J. Vac. Sci. Technol. B* **28**(2), 423–434 (2010).
- ¹⁵M. V. Moghaddam, P. Yaghoobi, G. A. Sawatzky, and A. Nojeh, *ACS Nano* **9**(4), 4064–4069 (2015).
- ¹⁶Z. J. Li, B. Bai, C. Li, and Q. Dai, *Carbon* **96**, 641–646 (2016).
- ¹⁷T. H. Wong, M. C. Gupta, and C. Hernandez-Garcia, *Nanotechnology* **18**(13), 135705 (2007).
- ¹⁸P. Yaghoobi, M. Michan, and A. Nojeh, *Appl. Phys. Lett.* **97**, 153119 (2010).
- ¹⁹S. Thomas, G. Wachter, C. Lemell, J. Burgdorfer, and P. Hommelhoff, *New J. Phys.* **17**, 063010 (2015).
- ²⁰S. Tsujino, F. le Pimpec, J. Raabe, M. Buess, M. Dehler, E. Kirk, J. Gobrecht, and A. Wrulich, *Appl. Phys. Lett.* **94**(9), 093508 (2009).
- ²¹Y. M. Li, W. Kim, Y. G. Zhang, M. Rolandi, D. W. Wang, and H. J. Dai, *J. Phys. Chem. B* **105**(46), 11424–11431 (2001).
- ²²M. Chhowalla, K. B. K. Teo, C. Ducati, N. L. Rupasinghe, G. A. J. Amaratunga, A. C. Ferrari, D. Roy, J. Robertson, and W. I. Milne, *J. Appl. Phys.* **90**(10), 5308–5317 (2001).
- ²³R. G. Hobbs, Y. Yang, A. Fallahi, P. D. Keathley, E. De Leo, F. X. Kartner, W. S. Graves, and K. K. Berggren, *ACS Nano* **8**(11), 11474–11482 (2014).
- ²⁴J. W. Gadzuk and E. W. Plummer, *Rev. Mod. Phys.* **45**(3), 487–548 (1973).
- ²⁵H. F. Ivey, *Phys. Rev.* **76**(4), 567–567 (1949).
- ²⁶R. G. Hobbs, Y. Yang, P. D. Keathley, M. E. Swanwick, L. F. Velasquez-Garcia, F. X. Kartner, W. S. Graves, and K. K. Berggren, *Nanotechnology* **25**(46), 465304 (2014).
- ²⁷W. A. Deheer, W. S. Bacs, A. Chatelain, T. Gerfin, R. Humphrey-Baker, L. Forro, and D. Ugarte, *Science* **268**(5212), 845–847 (1995).